



Cite this: *Org. Biomol. Chem.*, 2014, **12**, 7100

Ratiometric fluorescence chemosensor based on tyrosine derivatives for monitoring mercury ions in aqueous solutions†

Ponnaboina Thirupathi, Ponnaboina Saritha (née Gudelli) and Keun-Hyeung Lee*

Ratiometric fluorescent chemosensors **1** and **2** were synthesized based on tyrosine amino acid derivatives with a pyrene fluorophore. **1** and **2** showed high selectivity for Hg(II) ions among 13 metal ions in aqueous solutions. Both **1** and **2** sensitively detected Hg(II) ions in aqueous solutions by ratiometric response without interference of any of the other tested metal ions including Cu(II), Cd(II), Pb(II), and Ag(I) ions. **1** and **2** had tight binding affinities ($5.72 \times 10^{13} \text{ M}^{-2}$, $1.15 \times 10^{13} \text{ M}^{-2}$) for Hg(II) with nano-molar detection limits. The binding mode was characterized with the help of organic spectroscopic data, which revealed that the methoxyphenyl moieties of **1** and **2** played a vital role in the coordination of Hg(II). The deprotonation of the sulfonamide group is not a critical process for the binding of mercury ions. The methoxyphenyl moiety, sulfonamide group, and the C-terminal amide moiety of **1** and **2** as ligands for Hg(II) played crucial roles in the stabilization of the 2 : 1 complexes.

Received 21st May 2014,
Accepted 17th July 2014
DOI: 10.1039/c4ob01044b
www.rsc.org/obc

Introduction

The design and synthesis of fluorescent chemosensors for the detection and quantification of low level of Hg(II) ions in aqueous solutions have received considerable attention because Hg(II) ions are the most toxic and hazardous among the various heavy and transitional metal (HTM) ions.^{1,2} Even low concentrations of Hg(II) ions in aqueous solutions could accumulated in crops, fish, and the human body and could cause a wide variety of diseases such as prenatal brain damage and serious cognitive and motion disorders.^{3,4}

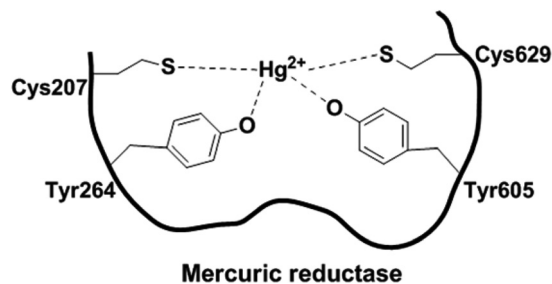
Several analytical techniques have been utilized for the detection of mercury ions, including atomic absorption/emission spectrometry, stripping voltammetry, and inductively coupled plasma mass spectrometry.^{1,5,6} These analytical techniques have shown some limitations such as tedious, time-consuming procedures and expensive instruments. Thus, an inexpensive and simple technique for monitoring Hg(II) ions has been highly demanded. In recent years, fluorescence techniques have received great attention because of inexpensive

instrumentation, high sensitivity, rapidity, and accurate detection.^{1,2,7} Thus, various types of fluorescence chemosensors for Hg(II) have been reported.⁸ The fluorescent chemosensors consist of a ligand-binding site (receptor), which is responsible for recognizing analytes and a signal transduction site (fluorophore), which converts the recognition events into fluorescent signals.^{8,9} The receptor part for specific target metal ions was conjugated with fluorophores for the synthesis of chemosensors for the metal ions. A variety of scaffolds such as thiacalixarene,^{8a} azines,^{8b} azadiene,^{8c} dioxaoctane-diamide,^{8d} cyclams,^{8ef} azacrown or azathiocrown,^{8g,h} thiocrown⁸ⁱ and azathia moieties,^{8j-p} have been utilized as receptors for the detection of Hg(II). Most of these receptors consisted of soft ligands, including nitrogen and sulfur for the coordination of Hg(II). However, most of these chemosensors have some limitations due to poor solubility in aqueous solutions, cross selectivity, low sensitivity, or interference with other heavy metal ions such as Cu(II), Cd(II), and Ag(I).^{8a-h,o,q} Therefore, the development of new chemosensors for selectively and sensitively monitoring Hg(II) in aqueous solutions is highly challenging.

In recent years, selective and sensitive detection of Hg(II) ions in aqueous solutions has been demonstrated with chemosensors based on amino acids containing soft ligands such as tryptophan and methionine.^{10,11} Recently, we synthesized a new chemosensor based on tyrosine, which showed a selective ratiometric response to Hg(II) ions in aqueous solution as well as in live cells.¹² The X-ray crystallographic study for mercuric reductase revealed that the tyrosine residue of the binding site acted as an important ligand for Hg(II) ions.¹³ Interestingly,

Bioorganic Chemistry Lab. Center for Design and Applications of Molecular Catalysts, Department of Chemistry and Chemical Engineering, Inha University, 253 Yonghyun-Dong, Nam-Gu, Incheon, 402-751, Korea. E-mail: leekh@inha.ac.kr

†Electronic supplementary information (ESI) available: Further experimental details, including (i) IR, ¹H NMR, ¹³C NMR, ESI mass, FAB-Mass, FAB-HRMS and UV-visible absorption spectra, (ii) UV-visible titration spectra, (iii) Job's plot, (iv) association constant, (v) detection limits, and (vi) ESI mass of 1-Hg(II) and 2-Hg(II) complex data of **1** and **2**. See DOI: 10.1039/c4ob01044b



Scheme 1 Schematic representation of the active binding site of mercuric reductase.¹²

even though the tyrosine moiety of the chemosensor did not contain soft ligands for the coordination of Hg(II), the chemosensor showed excellent selectivity and sensitivity for Hg(II) in aqueous solutions. On the other hand, the binding mode of this chemosensor was not fully understood in the following areas: (1) whether the hydroxyl group of the tyrosine moiety of the chemosensor would directly interact with Hg(II) or not because the oxide form of tyrosine in the mercuric reductase directly interacted with Hg(II) ions in the X-ray crystallographic study, as shown in Scheme 1,¹³ and (2) whether the deprotonation process of the sulfonamide group of the chemosensor might or might not be critical for the binding of Hg(II) because some studies about chemosensors suggested that the deprotonation process of the sulfonamide group might be important for the binding of Hg(II).^{10,11}

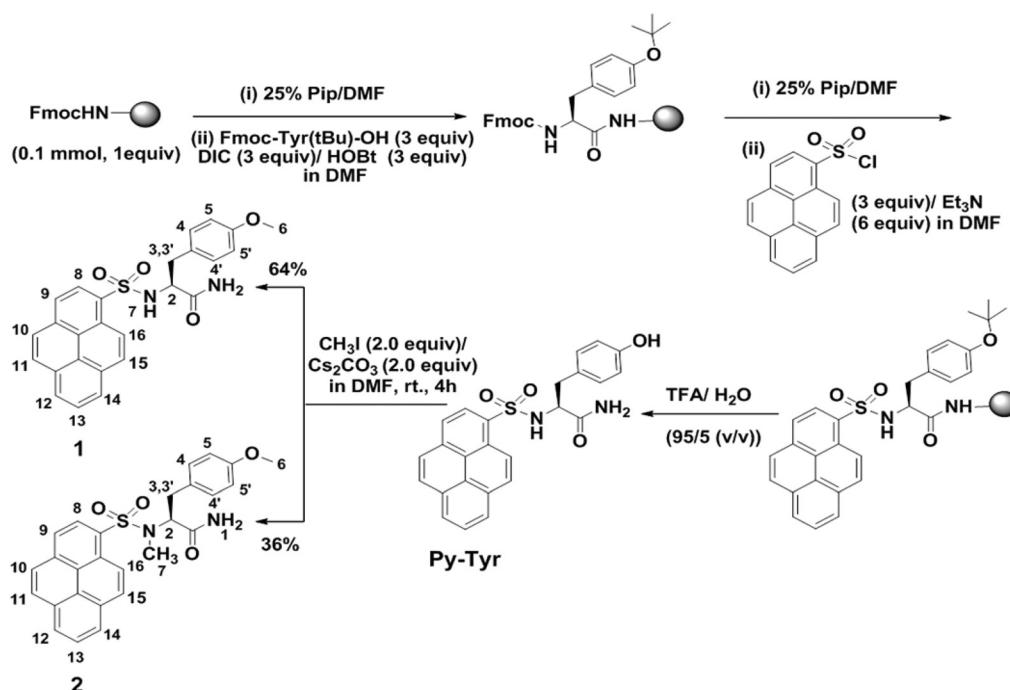
To answer these questions about the binding mode and to design new selective chemosensors for Hg(II), we synthesized

new chemosensors **1** and **2** based on tyrosine derivatives (Scheme 2). Interestingly, both chemosensors selectively detected Hg(II) ions in aqueous solution by ratiometric response and the binding mode of these chemosensors demonstrated a unique function of the aromatic and sulfonamide moieties as ligand binding sites for the coordination of mercury ions, stabilizing a 2 : 1 complex between the chemosensors and Hg(II).

Results and discussion

Solid phase synthesis and characterization of **1** and **2**

As shown in Scheme 2, pyrene-labelled tyrosine derivatives were easily synthesized by solid phase synthesis using Fmoc chemistry.¹⁴ Among the various fluorophores, pyrene was selected as a fluorophore because of its good photophysical properties such as high fluorescence quantum yield, chemical stability, and long fluorescence lifetime.^{15a-c} Moreover, pyrene shows monomer and excimer emissions depending on the proximity between the pyrene fluorophores.^{15d} The intensity ratio of the excimer emission to the monomer emission is sensitive to the distance between two pyrene fluorophores,^{15a,d} which makes ratiometric detection of target molecules possible if the chemosensor will form a 2 : 1 complex with the target molecules. The yields of pyrene-labeled Tyr derivatives, (PySO₂-Tyr(OCH₃)-NH₂, **1**) and (PySO₂(OCH₃)-Tyr(OCH₃)-NH₂, **2**) were 64% and 36%, respectively. The experimental procedure for the synthesis and characterization of **1** and **2** are described in the experimental procedure section (Fig. S1–S14†).



Scheme 2 Synthetic route for synthesis of chemosensors **1** and **2**.

Fluorescence emission optimization studies with Hg(II)

The stock solutions of **1** (1.24×10^{-3} M) and **2** (1.05×10^{-3} M) were prepared in DMSO–H₂O (1 : 1, v/v) and stored in a cold and dark place. The UV-Visible absorption spectra of both **1** and **2** elicit a typical pyrene absorption band at 353 nm in H₂O–DMSO (95 : 5, v/v, 10 mM HEPES) at pH 7.4 (Fig. S15†).

The responses of **1** and **2** to Hg(II) ions were characterized by fluorescence spectroscopy in a mixed organic-aqueous solution at pH 7.4. The fluorescent emission response of **1** (30 μ M) to Hg(II) ions was investigated in aqueous solutions (10 mM HEPES, pH 7.4) containing different volumes of DMSO (Fig. 1). Interestingly, the fluorescence behavior of **1** was dependent on the volume percentage of DMSO. The fluorescence emission spectrum of free **1** measured in aqueous solution containing 0.1% DMSO displayed a strong excimer emission at 490 nm, originating from the π - π stacking between two pyrene moieties, and weak monomer emissions at 386 and 400 nm. Upon increasing the percentage of DMSO in aqueous solution (10 mM HEPES at pH 7.4), a decrease in the excimer emission and a considerable increase in the monomer emissions were observed. The higher percentages of DMSO (>50%) in aqueous solution (10 mM HEPES at pH 7.4) induced a strong monomer emission intensity and a very weak excimer emission intensity for free **1**.

Upon addition of Hg(II) (2.5 equiv.), the enhancement of the excimer emission and concomitant decrease of the monomer emission were observed in aqueous solutions containing 0.1%,

3%, 5%, and 20% DMSO. Chemosensor **1** showed a significant ratiometric response to Hg(II) in these solvent conditions. However, a negligible enhancement of the excimer emission and a small decrease in the monomer emission were induced by Hg(II) in the aqueous solution containing 50% DMSO. There was no considerable change in the fluorescent spectrum in 100% DMSO solution. This indicates that the formation of a 2 : 1 complex between **1** and Hg(II) depends on the solvent polarity and hydrophobic interactions played an important role in the formation of this 2 : 1 complex. Considering the ratiometric response to Hg(II), the aqueous solution containing 5% DMSO (H₂O–DMSO, 95 : 5, v/v, 10 mM HEPES at pH 7.4) was chosen as the solvent system for further studies.

Fluorescence emission response to metal ions

As shown in Fig. 2, the fluorescence emission spectra of **1** in the absence of metal ions in aqueous solution displayed typical emission intensities at 386 and 400 nm, which are attributed to the pyrene monomeric emission (H₂O–DMSO, 95 : 5, v/v, 10 mM HEPES at pH 7.4). Upon addition of Hg(II), the monomer emission intensities at 386 and 400 nm decreased considerably and a concomitant increase of the pyrene excimer emission at 490 nm was observed. Interestingly, chemosensor **1** did not show any response to other tested metal ions, including Na(I), K(I), Mg(II), and Al(III) as a chloride anion and Ca(II), Co(II), Cr(III), Fe(III), Cu(II), Cd(II), Pb(II), Ag(I) and Zn(II) as a perchlorate anion.

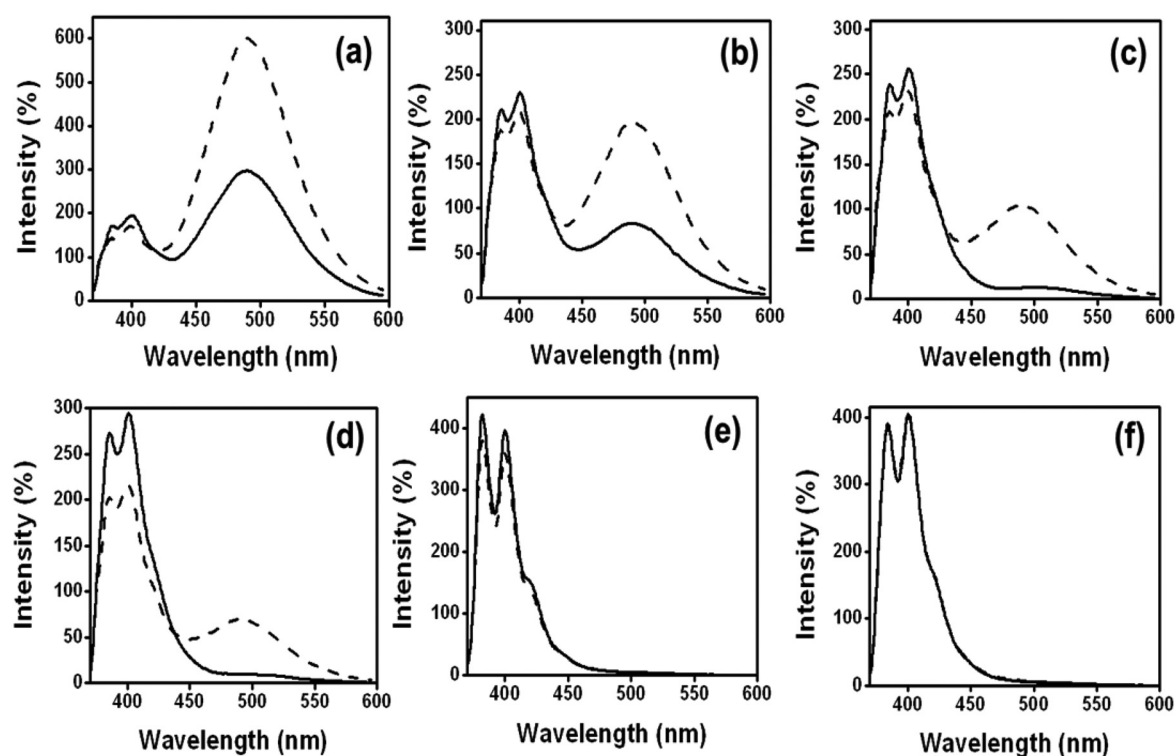


Fig. 1 Fluorescence emission intensity of **1** (30 μ M) in the absence (—) and presence (----) of 2.5 equiv. of Hg(II) in aqueous solution (10 mM HEPES, pH 7.4) containing DMSO (v/v) in amounts of (a) 0.1%, (b) 3%, (c) 5%, (d) 20%, (e) 50% and (f) 100%; λ_{ex} = 353 nm and slit = 15/5.0.

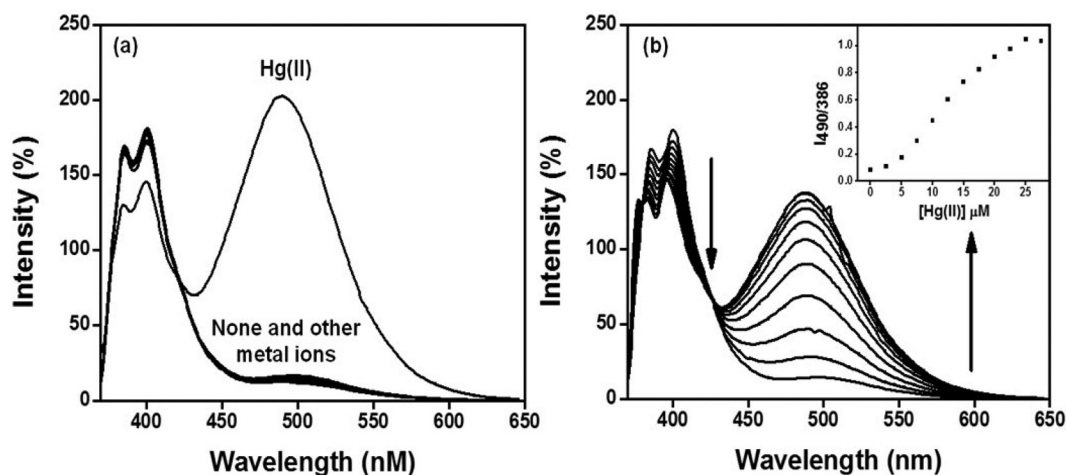


Fig. 2 Fluorescence emission spectra of **1** (40 μM) (a) in the presence of various metal ions (40 μM) and Na(I), K(I), Mg(II), and Mg(II) (2 mM), (b) upon gradual addition of Hg(II) (0, 0.0625, 0.125, 0.1875, 0.250, 0.3125, 0.375, 0.4375, 0.500, 0.5625, 0.625, and 0.6875 equiv.) to the aqueous solution (H_2O –DMSO, 95 : 5, v/v, 10 mM HEPES at pH 7.4), λ_{ex} = 353 nm, slit 15/5).

Fig. 2b exhibits the gradual emission intensity changes of **1** upon addition of Hg(II). The gradual addition of Hg(II) to the solution containing **1** resulted in a considerable decrease in the pyrene monomer emission intensities at 386 and 400 nm and a concomitant increase in the pyrene excimer emission at 490 nm. This was mainly due to the pyrene dimerization (π – π stacking) of the chemosensors in the presence of Hg(II). The intensity ratio (I_{490}/I_{386}) between the excimer and monomer emissions changed from 0.085 to 1.047 (*ca.* 12.3-fold enhancement) upon the addition of about 0.6 equiv. of Hg(II) (Fig. 2b, inset). Similarly, **2** also showed a selective ratiometric response to Hg(II) from among the various tested metal ions (Fig. 3a). The intensity ratio (I_{486}/I_{385}) between the excimer and monomer emissions was enhanced by 6.45-fold. About 0.75 equiv. of Hg(II) was required for saturation of the intensity

ratio change (Fig. 3b, inset). These results suggested that both **1** and **2** showed sensitive and selective ratiometric responses to Hg(II) in aqueous solution (H_2O –DMSO, 95 : 5, v/v, 10 mM HEPES at pH 7.4).

The pyrene dimerization of chemosensors **1** and **2** in the presence of Hg(II) was further confirmed by UV-Visible absorption (Fig. S16†). The absorbance band at 353 nm decreased with the gradual addition of Hg(II). This was due to the formation of a dimer between two pyrene moieties in the ground state in the presence of Hg(II).^{10b,11b,12}

Binding stoichiometry and binding affinity

We investigated the binding stoichiometry between the chemosensors (**1** and **2**) and Hg(II) by using Job's plot analysis (Fig. S17†). A maximum intensity around at 0.4 mole fraction

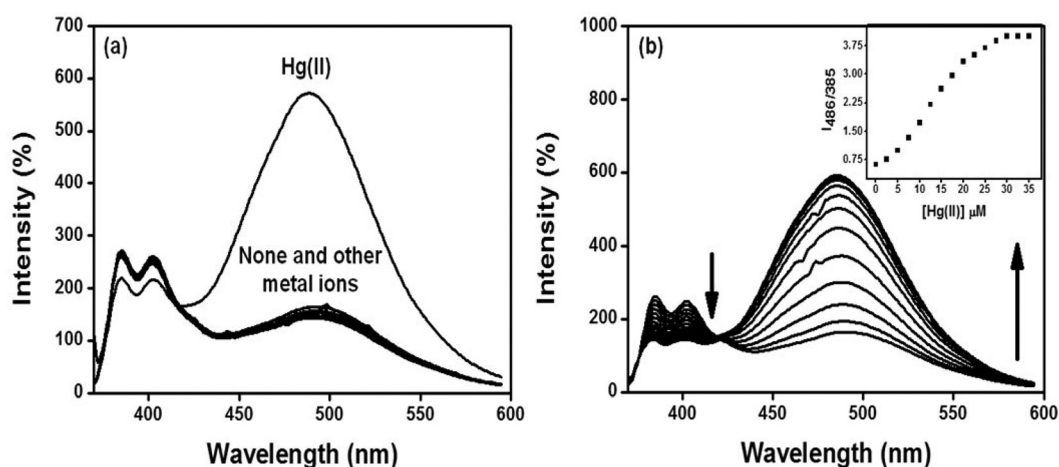


Fig. 3 Fluorescence emission spectra of **2** (40 μM) (a) in the presence of various metal ions (40 μM) and Na(I), K(I), Mg(II), and Mg(II) (2 mM), (b) upon gradual addition of Hg(II) (0, 0.0625, 0.125, 0.1875, 0.250, 0.3125, 0.375, 0.4375, 0.500, 0.5625, 0.625, 0.6875, 0.75, 0.8125, and 0.875 equiv.) to the aqueous solution (H_2O –DMSO, 95 : 5, v/v, 10 mM HEPES at pH 7.4; λ_{ex} = 353 nm, slit 15/6).

in the Job's plot analysis indicates that both **1** and **2** may form a 2 : 1 complex with Hg(II) in aqueous solution (H₂O–DMSO, 95 : 5, v/v, 10 mM HEPES at pH 7.4). By assuming 2 : 1 complex formation, the association constants (K_a) of **1** and **2** for Hg(II) were calculated as $5.72 \times 10^{13} \text{ M}^{-2}$ ($R^2 = 0.95$) and $1.15 \times 10^{13} \text{ M}^{-2}$ ($R^2 = 0.97$), respectively (Fig. S18†).^{12,16} The values clearly indicate that **1** and **2** have potent binding affinities for Hg(II) in aqueous solution. The sensitivities of **1** and **2** for Hg(II) were determined based on the linear relationships between the maximum monomer emission intensity at 386 nm and the concentration of Hg(II) (Fig. S19†). The detection limits were calculated to be 22.2 nM ($R^2 = 0.99$) and 44.0 nM ($R^2 = 0.99$) for **1** and **2**, respectively, by using $3\sigma/m$ where σ was the standard deviation of the blank measurements and m was the slope (sensitivity) of the intensity at 386 nm versus the concentration of Hg(II) in the plot. The results indicate that **1** is more sensitive than **2**. Both chemosensors **1** and **2** can be useful to detect qualitatively low levels of Hg(II) in aqueous solution.

Interference effect of other metal ions on fluorescence emission

As shown in Fig. 4, we investigated the interference effects of other metal ions on the detection ability of chemosensors **1** and **2** for Hg(II). The emission intensity ratios for **1** and **2** in the presence of Hg(II) were not considerably affected by the presence of high concentrations (2 mM) of Group I, II, and III metal ions such as Na(I), Mg(II), and Al(III). The intensity ratios for **1** and **2** in the presence of Hg(II) were not changed by other transition metal ions (1 equiv.). Interestingly, the heavy and transition metal (HTM) ions such as Ag(I), Pb(II), Cd(II), Zn(II), and Cu(II) (1 equiv.) did not interfere with the detection of Hg(II) by **1** and **2**. Most of the reported chemosensors for Hg(II) suffered from cross sensitivity with other heavy and transition metal ions such as Cu(II), Ag(I), Cd(II), and Pb(II).^{8a–h,o,q,11b} whereas both **1** and **2** were highly selective for Hg(II) among other metal ions.

Fluorescence emission studies at different pH

The ratiometric responses of **1** and **2** to Hg(II) were examined at different pH levels to investigate the working pH range of the chemosensors and the role of the functional groups of **1** and **2** for the binding of Hg(II). The detection of HTM ions in acidic conditions is highly desirable because the solubility of HTM ions may increase in acidic conditions; therefore, the contamination of HTM ions to environment is more serious in acidic conditions. However, many of the reported chemosensors, including ratiometric fluorescent chemosensors, were not able to detect Hg(II) ions in acidic conditions. This was mainly due to the inhibition of the PET or ICT process for sensing the metal ions by the protonation of the amine group of the chemosensors in acidic conditions.^{8b–f,9}

As shown in Fig. 5, both **1** and **2** showed considerable ratiometric responses to Hg(II) at an acidic pH. The emission intensity ratio increased from 0.08 to 0.34 for **1** and 0.54 to 1.02 for **2** in the presence of Hg(II). Under basic conditions (pH = 10.5 or 11.5), **1** displayed a ratiometric response to Hg(II). The emission intensity ratio (I_{490}/I_{386}) of **1** increased from 0.1 to 3.4 in the presence of Hg(II) at pH 10.5, whereas the intensity ratio increased from 0.09 to 3.1 at pH 11.5. The deprotonated sulfonamide group ($pK_a \approx 10$) did not considerably affect the ratiometric response to Hg(II).^{10d,11c} Under basic conditions, chemosensor **2** also showed a ratiometric response to Hg(II). Even though **2** contains an *N*-methyl sulfonamide group and it showed a more enhanced excimer emission in the presence of Hg(II) than **1**, the intensity ratio change of **2** (from 0.28 to 2.82) induced by Hg(II) was slightly lower than that of **1**. The pH titration experiment reveals that **1** and **2** are suitable for monitoring Hg(II) by ratiometric response over a wide range of pH values (pH 4.5–11.5).

Binding mode of **1** and **2** with Hg(II)

The binding mode of the chemosensor with Hg(II) was investigated by using ESI⁺ mass spectrometry. When 1.0 equiv. of

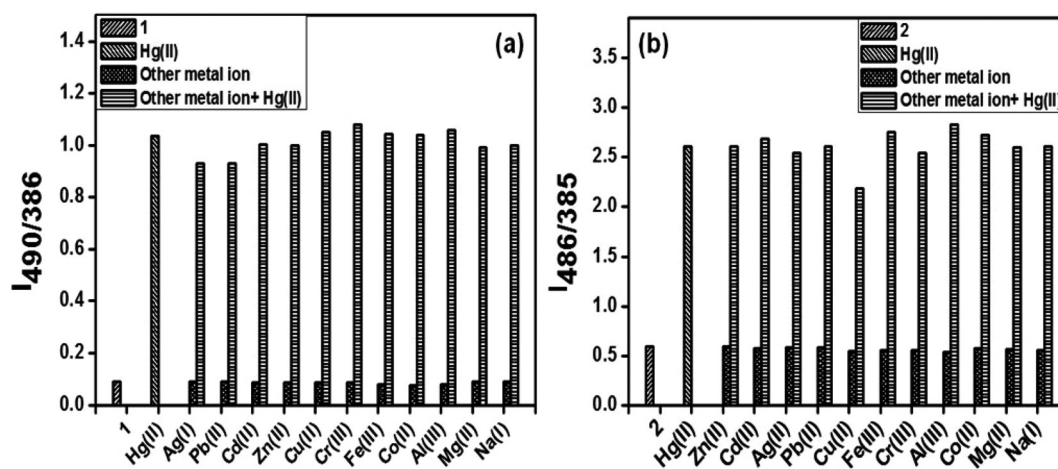


Fig. 4 Fluorescence emission intensity ratio of (a) **1** (I_{490}/I_{386} , 40 μM , slit 15/5) and (b) **2** (I_{486}/I_{385} , 40 μM , slit 15/6) in the presence various other metal ions and of Hg(II) (1 equiv.) in aqueous solution (H₂O–DMSO, 95 : 5, v/v, 10 mM HEPES at pH 7.4). The concentrations of Group I, II, and III metal ions were 2 mM, and the concentrations of other metal ions were 40 μM .

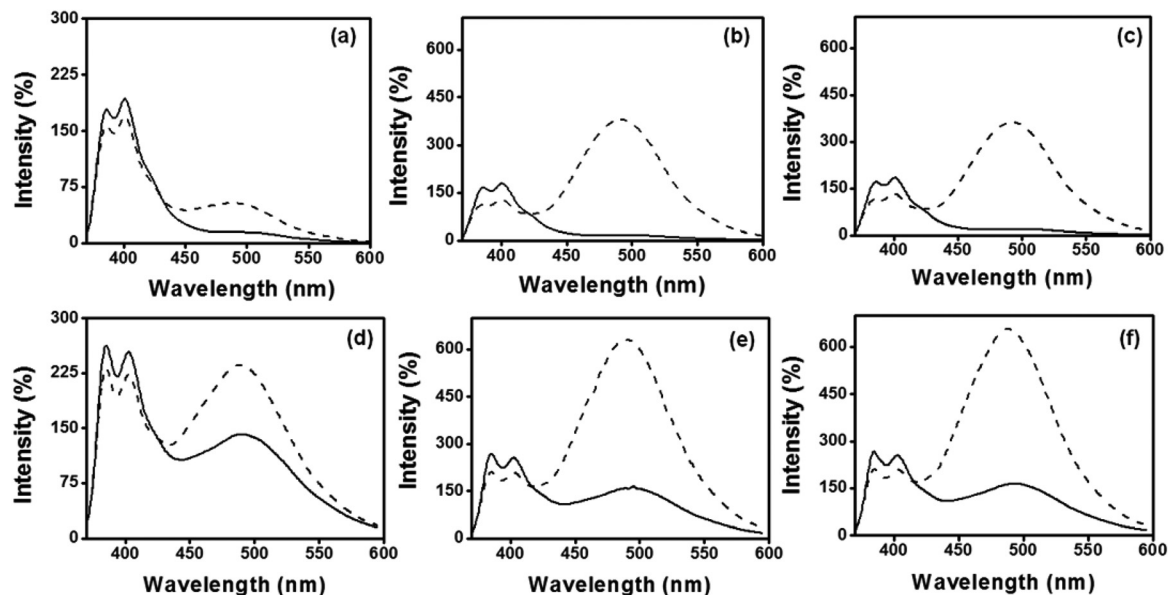


Fig. 5 Fluorescence spectra of **1** (40 μM) in the absence (—) and presence (-----) of Hg(II) (1.0 equiv.) at pH (a) 4.5, (b) 10.5, and (c) 11.5 and fluorescence spectra of **2** (40 μM) in the absence (—) and presence (-----) of Hg(II) (1.0 equiv.) at pH (d) 4.5, (e) 10.5, and (f) 11.5.

Hg(II) was added to the solution of **1** (500 μM), a new peak appeared at 1114.74 (m/z) corresponding to $[(2\cdot 1) + \text{Hg}^{2+} - \text{H}^+]^+$ (Fig. S20†). This result clearly suggests that **1** may form a 2 : 1 complex with Hg(II) . Similarly, chemosensor **2** may also form a 2 : 1 complex upon addition of 1.0 equiv. of Hg(II) because the peak at 1145.09 (m/z) corresponding to $[(2\cdot 2) + \text{Hg}^{2+} - \text{H}^+]^+$ appeared (Fig. S21†). The result suggests that both chemosensors may form a 2 : 1 complex.

^1H NMR titration experiments provided additional information for the detailed binding modes of **1** and **2** with Hg(II) . ^1H NMR spectra were recorded in D_2O - DMSO-d_6 (8 : 2, v/v) at pH 7.5 adjusted with 1% NaOD because both chemosensors exhibited much better ratiometric response to Hg(II) in neutral and basic pH rather than acidic pH. As depicted in Fig. 6, the ^1H NMR spectra of **1** was recorded with an increased amount of Hg(II) and displayed the downfield shift ($\Delta 0.02$ and $\Delta 0.05$ ppm) of proton signals at H-4,4' and H-5,5', corresponding to the methoxyphenyl moiety. These shifts were attributed to the coordination of Hg(II) with the methoxyphenyl moiety of **1**. The downfield shift ($\Delta 0.04$ ppm) of the proton signal (H-8) at 8.64 ppm of the pyrene near (*ortho*) to the sulfonamide group was due to the interactions between Hg(II) and the sulfonamide group. Subsequently, all the other aromatic protons of pyrene were also slightly downfield shifted upon binding with Hg(II) .

As shown in Fig. 7, the binding mode of **2** and Hg(II) was also investigated by ^1H NMR titration. After the addition of 1 equiv. Hg(II) , downfield shifts ($\Delta 0.05$ and $\Delta 0.07$ ppm) of proton signals were induced for H-4,4' and H-5,5', corresponding to the methoxyphenyl protons. This indicates that Hg(II) may strongly chelate the methoxyphenyl moiety of **2**. The slightly downfield shifts of all the aromatic protons in pyrene were also observed in the presence of Hg(II) . This may be due to the

interactions of the *N*-methyl sulfonamide group with Hg(II) . This result strongly suggests that the deprotonation process is not an important criterion for the binding of Hg(II) ions. The ^1H NMR spectra indicate that the methoxyphenyl and sulfonamide moieties acted as ligands for coordination of Hg(II) . The C-terminal amide proton peaks of the **1** and **2** could not be observed due to D_2O in this solvent system; however, the previous results about chemosensors based on amino acids suggest that the C-terminal amide group plays an important role in the binding of target metal ions.^{10b,11a}

Chemosensor **1** showed a potent binding affinity for Hg(II) compared to **2** in aqueous solution. The association constants (K_a) of **1** and **2** for Hg(II) were $5.72 \times 10^{13} \text{ M}^{-2}$ and $1.15 \times 10^{13} \text{ M}^{-2}$, respectively. These values clearly indicate that **1** and **2** have more potent binding affinities for Hg(II) than the previously reported chemosensor (**Py-Tyr**) based on tyrosine (K_a , $3.5 \times 10^{12} \text{ M}^{-2}$) in aqueous solution.¹² These results clearly suggest that the oxide form of the tyrosine moiety of **Py-Tyr** may not directly interact with Hg(II) like the binding mode elucidated in the X-ray crystallographic study.¹³ Furthermore, the more potent binding affinity of **1** than that of **Py-Tyr** strongly suggests that the methoxyphenyl moiety of **1** is an important ligand, which may chelate Hg(II) . Interestingly, chemosensor **2**, which contains an *N*-methyl sulfonamide group ($-\text{SO}_2-\text{NCH}_3-$), showed a similar binding affinity to that of chemosensor **1**, which contains a sulfonamide group. This suggests that the deprotonation process is not crucial for the binding of Hg(II) ions. The binding mode of both **1** or **2** with Hg(II) was proposed based on fluorescent and UV-visible spectra, pH titration results, ESI-mass spectra, ^1H NMR titration results, and the previously reported binding modes of chemosensors based on amino acids.^{10b,11a} As shown in Scheme 3, the chemosensors formed a 2 : 1 complex with Hg(II) by chelation of the

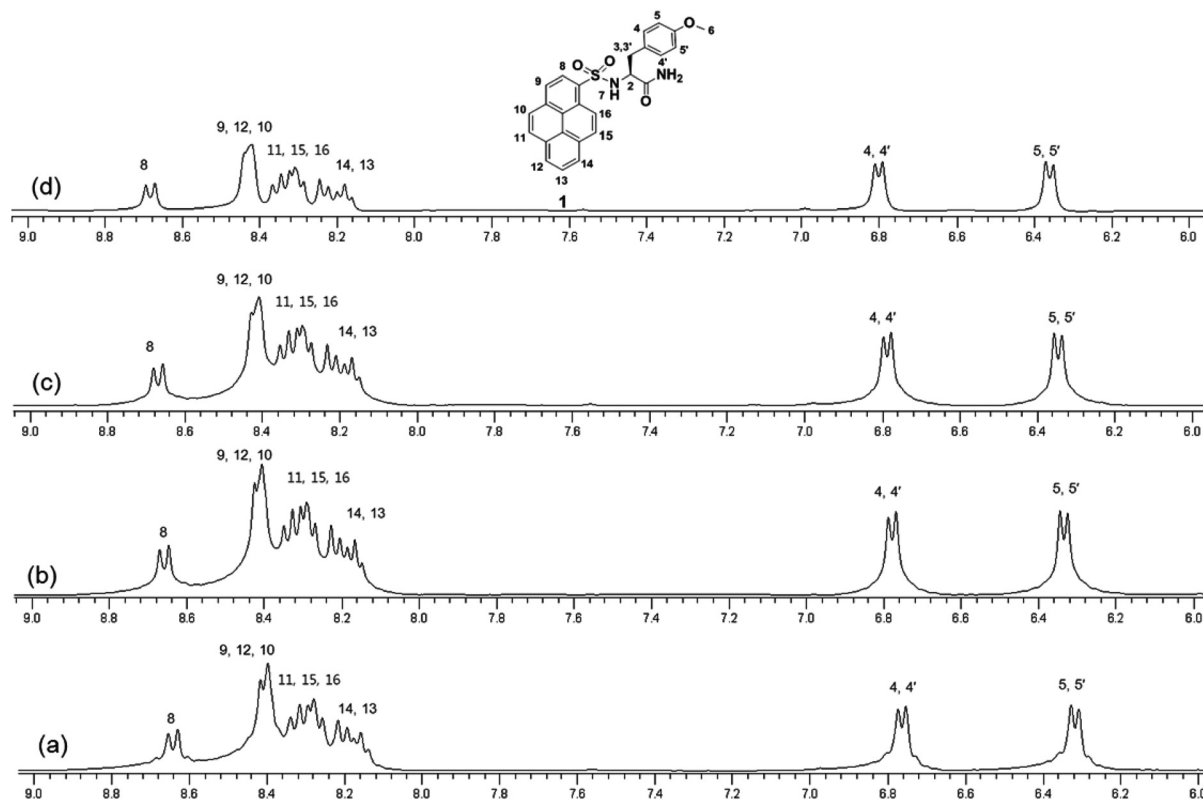


Fig. 6 Partial ^1H NMR spectra (400 MHz) of chemosensor **1** (8.4 mM) with (a) 0 equiv. of $\text{Hg}(\text{ClO}_4)_2$, (b) 0.25 equiv. of $\text{Hg}(\text{ClO}_4)_2$, (c) 0.50 equiv. of $\text{Hg}(\text{ClO}_4)_2$, and (d) 1 equiv. of $\text{Hg}(\text{ClO}_4)_2$ in D_2O – $\text{DMSO}-d_6$ (8 : 2, v/v, pH \approx 7.5).

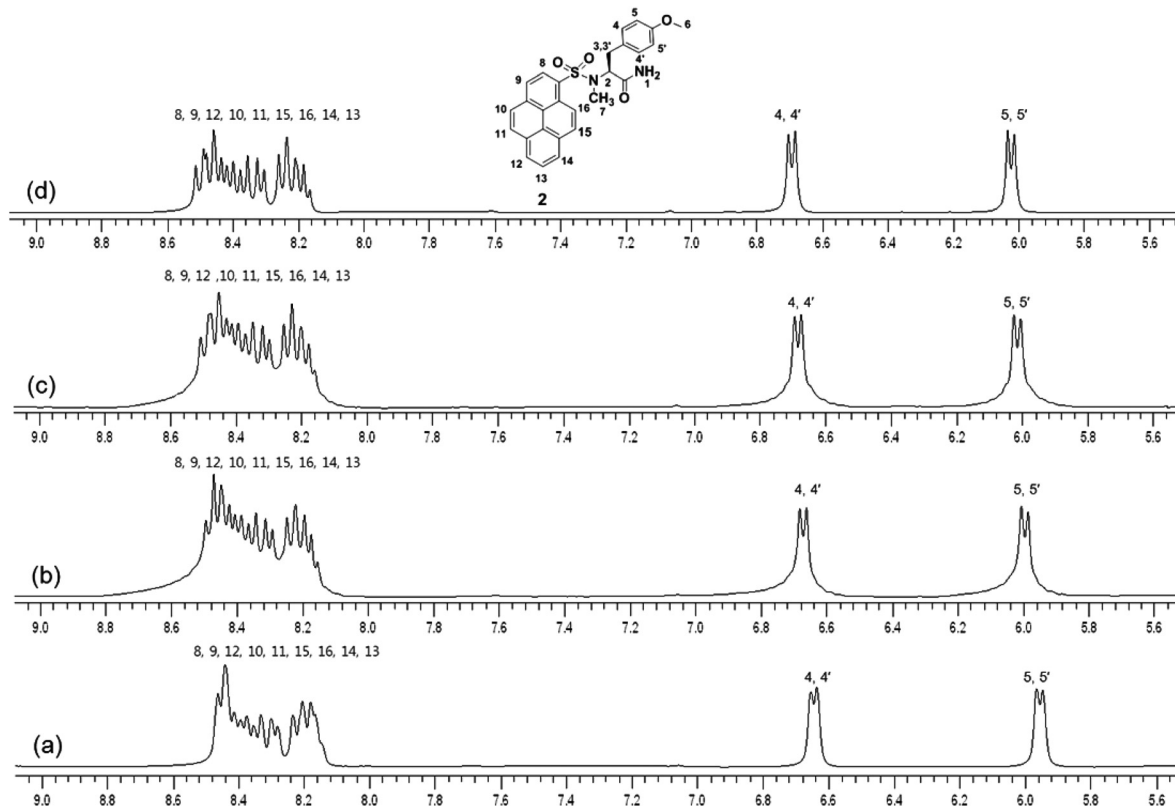
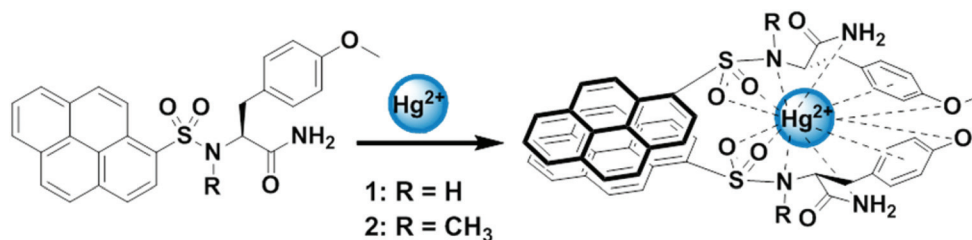


Fig. 7 Partial ^1H NMR spectra (400 MHz) of chemosensor **2** (8.7 mM) in (a) 0 equiv. of $\text{Hg}(\text{ClO}_4)_2$, (b) presence of 0.25 equiv., (c) presence of 0.50 equiv., and (d) presence of 1 equiv. of $\text{Hg}(\text{ClO}_4)_2$ in D_2O – $\text{DMSO}-d_6$ (8 : 2, v/v, \sim pH = 7.5).



Scheme 3 A proposed binding mode of chemosensor 1 or 2 with Hg(II).

sulfonamide group, the amide group, and the methoxyphenyl moiety. Hg(II) may interact with the methoxyphenyl moiety by cation- π interactions and with the methoxy as an electron donating group from the increased electron density of the aromatic part. The binding mode was consistent with the binding mode proposed by Li *et al.* using an X-ray crystal structure between dansyl-tryptophanmethyl ester and Hg(II)^{11a} in which the sulfonamide and ester groups of the chemosensor were important ligands for stabilizing a 2 : 1 complex between the chemosensor and Hg(II).

Conclusions

Chemosensors **1** and **2** based on tyrosine derivatives selectively detected Hg(II) ions in aqueous solution by ratiometric response. **1** and **2** had potent binding affinities ($5.72 \times 10^{13} \text{ M}^{-2}$ and $1.15 \times 10^{13} \text{ M}^{-2}$) for Hg(II) in aqueous solutions and the sensitive ratiometric response to Hg(II) was not interfered with by any of the other tested metal ions, including Ag(I), Pb(II), and Cu(II). The detection limits of **1** and **2** for Hg(II) in aqueous solutions were determined to be 22.2 nM and 44.0 nM, respectively. The methoxyphenyl moiety of **1** or **2** played a vital role in the coordination of Hg(II). The deprotonation of the sulfonamide group ($-\text{SO}_2-\text{NH}-$) was not a critical process for the binding of mercury ions. The methoxyphenyl moiety, sulfonamide group, and the C-terminal amide moiety of **1** and **2** as ligands for Hg(II) played crucial roles in the stabilization of the 2 : 1 complex.

Experimental section

Reagents

Rink Amide MBHA resin, Fmoc-Tyr(*t*Bu)-OH, *N,N*-diisopropylcarbodiimide (DIC), and 1-hydroxybenzotriazole (HOBt) were purchased from Bead Tech. Other reagents for solid phase synthesis, including trifluoroacetic acid (TFA), triethylamine, *N,N*-dimethylformamide (DMF), piperidine, cesium carbonate (Cs_2CO_3), iodomethane (CH_3I), and anhydrous sodium sulfate (Na_2SO_4) were purchased from Aldrich. 1-Pyrenesulfonyl chloride was synthesized from 1-pyrenesulfonic acid (purchased from Aldrich).

Solid phase synthesis: General experimental procedure

Py-Tyr was efficiently synthesized in solid-phase synthesis with 9-fluorenylmethoxycarbonyl (Fmoc) chemistry (Scheme 1).¹³ Diisopropylcarbodiimide (DIC) and 1-hydroxybenzotriazole (HOBt) *in situ* activation method was used for the coupling reactions. Fmoc-Tyr(*t*Bu)-OH (0.3 mmol, 0.3 equiv.) was loaded to Rink Amide MBHA (0.1 mmol, 0.1 equiv.) according to the reported procedure. After washing, drying, and deprotecting the Fmoc group with 25% piperidine in *N,N*-dimethylformamide (DMF). The 1-pyrenesulfonyl chloride (0.3 mmol, 0.3 equiv.) was then coupled with the deprotected amino group in the presence of triethylamine (0.6 mmol, 0.6 equiv.). Finally, the cleavage of **Py-Tyr** from the resin was accomplished with $\text{CF}_3\text{COOH}-\text{H}_2\text{O}$ (TFA-water, 95/5, v/v) at room temperature for 3 h. Following vacuum filtration and removal of TFA with N_2 blow-off, the crude product was precipitated from cold ether. The solid precipitate was centrifuged, washed with ether, and lyophilized under vacuum. The crude product was used for further synthesis of **1** and **2** in the solution phase.

To a stirred solution of **Py-Tyr** in dry DMF (1.5 mL), 0.2 equiv. cesium carbonate (Cs_2CO_3) was added under nitrogen atmosphere at 0 °C. The reaction mixture was stirred for 10 min at room temperature and 0.2 equiv. iodomethane (CH_3I) dissolved in dry DMF (0.5 mL) was slowly added by drop by drop. After 4 h, the reaction mixture was filtered, and the residue was washed with DMF. To the filtrate, 2 mL of water was added and extracted with ethyl acetate ($3 \times 3 \text{ mL}$). The collected ethyl acetate portions were dried over anhydrous Na_2SO_4 and concentrated under vacuum. The crude product was purified with semi preparative HPLC using water (0.1% TFA)-acetonitrile (0.1% TFA) gradient. The retention times of **1** and **2** are 52 and 60 min, respectively. Compounds **1** and **2** were characterized by IR, ^1H and ^{13}C NMR and ESI-mass data. The melting point, IR, ^1H NMR, ^{13}C NMR, and ESI-mass data of **1** and **2** are given below.

Compound 1. White solid, mp 255–256 °C; IR (KBr): 3448, 3328 (br s) 2917, 1680, 1510, 1323, 1120 cm^{-1} ; ^1H NMR (400 MHz, $\text{DMSO}-d_6$) δ 9.05 (s, 1H), 8.79 (d, $J = 8.4 \text{ Hz}$, 1H), 8.47–8.42 (m, 3H), 8.39–8.34 (m, 3H), 8.26 (d, $J = 8.4 \text{ Hz}$, 1H), 8.18 (t, $J = 8.4 \text{ Hz}$, 1H), 7.48 (br s, 1H), 7.00 (br s, 1H), 6.88 (d, $J = 8.6 \text{ Hz}$, 2H), 6.46 (d, $J = 8.6 \text{ Hz}$, 2H), 4.74 (t, $J = 8.5 \text{ Hz}$, 1H), 3.01 (s, 3H), 2.89 (dd, $J = 12.0, 2.0 \text{ Hz}$, 1H); 2.61 (dd, $J = 12.0, 1.8 \text{ Hz}$, 1H); ^{13}C NMR (100 MHz, $\text{DMSO}-d_6$) δ 171.61, 155.8, 134.1, 131.3, 130.5, 130.1, 129.8, 129.6, 129.5, 127.5, 127.1, 127.0,

126.9, 126.8, 124.3, 124.0, 123.3, 123.1, 114.9, 59.4, 34.5, 30.4; ESI-Mass (m/z): $[M + H]^+$ at 459.18; HRMS-FAB (m/z): $[M + H]^+$ calculated for $C_{26}H_{23}N_2O_4S$: 459.1379, observed: 459.1373.

Compound 2. White solid, mp 154–155 °C; IR (KBr): 3443, 2939, 1679, 1509, 1241, 1120 cm^{-1} ; 1H NMR (400 MHz, $DMSO_6$) δ 8.59 (d, J = 8.6 Hz, 1H), 8.50–8.43 (m, 1H), 8.43–8.37 (m, 2H), 8.36–8.31 (m, 2H), 8.28–8.23 (m, 2H), 8.21–8.15 (m, 1H), 7.54 (br s, 1H), 7.07 (br s, 1H), 6.78 (d, J = 8.4 Hz, 2H), 6.17 (d, J = 8.4 Hz, 2H), 4.65–4.61 (m, 1H), 3.17 (s, 3H), 3.12 (s, 3H), 2.89 (dd, J = 12.8, 2.0 Hz, 1H), 2.68 (dd, J = 12.8, 1.8 Hz, 1H); ^{13}C NMR (100 MHz, $DMSO_6$) δ 172.0, 157.2, 134.1, 131.2, 130.5, 130.0, 129.5, 129.3, 129.2, 128.3, 127.4, 127.3, 126.9, 126.7, 124.3, 123.8, 123.1, 112.2, 112.8, 59.3, 54.2, 34.3, 30.4; ESI-Mass (m/z): $[M + H]^+$ at 473.19; HRMS-FAB (m/z): $[M + H]^+$ calculated for $C_{27}H_{25}N_2O_4S$: 473.1535, observed: 473.1530.

General fluorescence measurements

The stock solutions of **1** (1.23×10^{-3} M) and **2** (1.05×10^{-3} M) were prepared in $DMSO-H_2O$ (1 : 1, v/v) and stored in a cold and dark place. This stock solution was used for all spectrofluorometric experiments after appropriate dilution. The fluorescence experiments were carried out using the above solution after setting the pH of the solution to 7.4 using a 10 mM HEPES buffer solution. The fluorescence emission spectrum of a sample in a 10 mm path length quartz cuvette was measured in 10 mM HEPES buffer solution at pH 7.4 using a Perkin Elmer luminescence spectrophotometer (model LS 55). Emission spectra (360–600 nm) of **1** and **2** in the presence of several metal ions (Na(I), K(I), Mg(II), Al(III) as a chloride anion, Ca(II), Co(II), Cr(III), Cu(II), Fe(III), Mn(II), Ni(II), Pb(II), and Zn(II) as a perchlorate anion) were measured by excitation at 352 nm. The slit sizes used for excitation and emission 15 and 5 nm for **1** and 15 and 6 nm for **2**. The concentrations of **1** and **2** were confirmed by UV absorbance at 342 nm for the pyrene group. The molar extension coefficient (ϵ) of **1** and **2** is $16\,000\,cm^{-1}\,M^{-1}$ at 342 nm.

Determination of association constant

The association constant for the 2 : 1 complex was calculated based on the titration curve of probes **1** and **2** with $Hg(II)$. Association constants were determined by a nonlinear least squares fitting of the data with the following equation as referenced elsewhere.^{10b,11b,12,16}

$$y = \frac{x}{2 \times a \times b \times (1 - x)^2} + \frac{x \times b}{2}$$

where x is $I - I_0/I_{max} - I_0$, y is the concentration of metal ions, a is the association constant, and b is the concentration of chemosensor.

Determination of detection limit

The detection limits were calculated based on the fluorescence titration. To determine the S/N ratio, the emission intensities of **1** and **2** without $Hg(II)$ were measured 10 times and the standard deviation of blank measurements was determined. Three

independent duplication measurements of emission intensity were performed in the presence of $Hg(II)$ and each average value of the intensities was plotted as a concentration of $Hg(II)$ to determine the slope. The detection limit is then calculated with the following equation.

$$\text{Detection limit} = 3\sigma/m$$

where σ is the standard deviation of blank measurements, m is the slope between intensity versus sample concentration.

Acknowledgements

This work was supported by a grant (2012R1AB3000574) from the Basic Research Program of the National Research Foundation and a grant (201200054 0013) from the Korea Environmental Industry and Technology Institute, and Dr Thirupathi also acknowledges the Department of Chemistry and Chemical Engineering, Inha University, Incheon, Republic of Korea.

References

- 1 E. M. Nolan and S. Lippard, *Chem. Rev.*, 2008, **108**, 3443.
- 2 H. N. Kim, W. X. Ren, J. S. Kim and J. Y. Yoon, *Chem. Soc. Rev.*, 2012, **41**, 3210.
- 3 (a) P. Grandjean, P. Weihe, R. F. White and F. Debes, *Environ. Res.*, 1998, **77**, 165; (b) EPA Mercury Update Impact on Fish Advisories, EPA Fact Sheet EPA-823-F-01-011, EPA, Office of Water, Washington, DC, 2001, pp. 1–10.
- 4 M. Harada, *Crit. Rev. Toxicol.*, 1995, **25**, 1.
- 5 K. Das, M. de la Guardia and M. L. Cervera, *Talanta*, 2001, **55**, 1.
- 6 S. K. Aggarwal, M. Kinter and D. A. Herold, *Clin. Chem.*, 1994, **40**, 1494.
- 7 J. R. Lakowicz, *Principles of Fluorescence Spectroscopy*, Kluwer Academic/Plenum, New York, 1999.
- 8 (a) V. Csokai, M. Kadar, D. L. H. Mai, O. Varga, K. Toth, M. Kubinyi, A. Grun and I. Bitter, *Tetrahedron*, 2008, **64**, 1058; (b) R. Martinez, A. Espinosa, A. Tarraga and P. Molina, *Org. Lett.*, 2005, **7**, 5869; (c) Y. Zhou, C.-Y. Zhu, X.-S. Gao, X.-Y. You and C. Yao, *Org. Lett.*, 2010, **12**, 2566; (d) J. S. Kim, M. G. Choi, K. C. Song, K. T. No, S. Ahn and S.-K. Chang, *Org. Lett.*, 2007, **9**, 1129; (e) P. Mahato, A. Ghosh, S. Saha, S. Mishra, S. K. Mishra and A. Das, *Inorg. Chem.*, 2010, **49**, 11485; (f) S. Voutsadaki, G. K. Tsikalas, E. Klontzas, G. E. Froudakis, S. A. Pergantis, K. D. Demadis and H. E. Katerinopoulos, *RSC Adv.*, 2012, **2**, 12679; (g) T. Chen, W. Zhu, Y. Xu, S. Zhang, X. Zhang and X. Qian, *Dalton Trans.*, 2010, **39**, 1316; (h) H. N. Lee, H. N. Kim, K. M. K. Swamy, M. S. Park, J. Kim, H. Lee, K. H. Lee, S. Park and J. Yoon, *Tetrahedron Lett.*, 2008, **49**, 1261; (i) M. Yuan, Y. Li, C. Li, X. Liu, J. Lv, J. Xu, H. Liu, S. Wang and D. Zhu, *Org. Lett.*, 2007, **9**, 2313; (j) E. M. Nolan and S. J. Lippard, *J. Am. Chem. Soc.*, 2003,

- 125, 14270; (k) E. M. Nolan and S. J. Lippard, *J. Mater. Chem.*, 2005, **15**, 2778; (l) E. M. Nolan and S. J. Lippard, *J. Am. Chem. Soc.*, 2007, **129**, 5910; (m) J. Huang, Y. Xu and X. Qian, *J. Org. Chem.*, 2009, **74**, 2167; (n) M. Taki, K. Akaoka, S. Iyoshi and Y. Yamamoto, *Inorg. Chem.*, 2012, **51**, 13075; (o) H. A. El-Shekheby, A. H. Mangood, S. M. Hamza, A. S. Al-Kady and E.-Z. M. Ebeid, *Luminescence*, 2014, **29**, 158; (p) J. Fan, K. Guo, X. Peng, J. Du, J. Wang, S. Sun and H. Li, *Sens. Actuators, B*, 2009, **142**, 191; (q) N. Wanichacheva, S. Watpathomsub, V. S. Lee and K. Grudpan, *Molecules*, 2010, **15**, 1798; (r) M. Zhu, M. Yuan, X. Liu, J. Xu, J. Lv, C. Huang, H. Liu, Y. Li, S. Wang and D. Zhu, *Org. Lett.*, 2008, **10**, 1481.
- 9 (a) B. Valeur and I. Leray, *Coord. Chem. Rev.*, 2000, **205**, 3; (b) A. P. DeSilva, H. Q. N. Gunaratne, T. Gunnlaugsson, A. J. M. Huxley, C. P. McCoy, J. T. Rademacher and T. E. Rice, *Chem. Rev.*, 1997, **97**, 1515.
- 10 (a) M. H. Yang, C. R. Lohani, H. J. Cho and K. H. Lee, *Org. Biomol. Chem.*, 2011, **9**, 2350; (b) M. H. Yang, P. Thirupathi and K. H. Lee, *Org. Lett.*, 2011, **13**, 5028; (c) A. Banerjee, D. Karak, A. Sahana, S. Guha, S. Lohar and D. Das, *J. Hazard. Mater.*, 2011, **186**, 738; (d) L. Chen, L. Yang, H. Li, Y. Gao, D. Deng, Y. Wu and L.-J. Ma, *Inorg. Chem.*, 2011, **50**, 10028.
- 11 (a) H. Li, Y. Li, Y. Dang, L. Ma, Y. Wu, G. Hou and L. Wu, *Chem. Commun.*, 2009, 4453; (b) L. N. Neupane, J. H. Park and K. H. Lee, *Org. Lett.*, 2013, **15**, 254; (c) C. R. Lohani, J. M. Kim and K. H. Lee, *Tetrahedron*, 2011, **67**, 4130; (d) C. R. Lohani, L. N. Neupane, J. M. Kim and K. H. Lee, *Sens. Actuators, B*, 2012, **161**, 1088.
- 12 D.-H. Kim, J. Seoung, H. Lee and K. H. Lee, *Sens. Actuators, B*, 2014, **196**, 421.
- 13 (a) N. Schiering, W. Kabsch, M. J. Moore, M. D. Distefano, C. T. Walsh and E. F. Pai, *Nature*, 1991, **352**, 168; (b) S. Engst and S. M. Miller, *Biochemistry*, 1998, **37**, 11496.
- 14 G. B. Fields and R. L. Noble, *Int. J. Pept. Protein Res.*, 1990, **35**, 161.
- 15 (a) F. M. Winnik, *Chem. Rev.*, 1993, **93**, 587; (b) C. Yao, H.-B. Kraatz and R. P. Steer, *Photochem. Photobiol. Sci.*, 2005, **4**, 191; (c) J. B. Birks, *Rep. Prog. Phys.*, 1975, **38**, 903; (d) P. Thirupathi and K. H. Lee, *Bioorg. Med. Chem.*, 2013, **21**, 7964.
- 16 Y. Kubo, M. Kato, Y. Misawa and S. Tokita, *Tetrahedron Lett.*, 2004, **45**, 3769.